Offset Tolerant Demodulator for Frequency/Phase Modulation in Time-Varying Channel

1st Siavash Safapourhajari
University of Twente
Enschede, Netherlands
s.safapourhajari@utwente.nl

2nd André B. J. Kokkeler
University of Twente
Enschede, Netherlands
a.b.j.kokkeler@utwente.nl

***Abstract*—Carrier frequency offset (CFO) and time-varying fading channels are two problems that emerging ultra-narrowband solutions for Internet of Things and Wireless Sensor Networks need to tackle. Previously, an offset tolerant demodulator for Double Differential PSK (DDPSK) has been proposed to overcome CFO. To combat channel distortion, time or frequency diversity together with coding techniques can be utilized. However, these necessitate transmitting extra bits and leads to an increase in packet time. A longer packet time corresponds to longer on-time of the RF front-end and more power consumption. To avoid longer packet for the same symbol rate, a higher order modulation is required which considerably degrades BER performance. In this work, instead of higher order DDPSK, hybrid frequency/phase modulation is used. An offset tolerant demodulator for hybrid modulation is proposed which provides the same robustness against CFO as DDPSK. Besides, it provides higher order of modulation with less performance loss compared to higher order DDPSK. Simulation results show that a combination of BFSK and QPSK using the proposed demodulator can achieve almost 4 dB improvement at BER=0.001 in a Rayleigh channel compared to Double Differential 8PSK (DD8PSK) which can provide the same modulation order.**

***Index Terms*—Frequency/Phase Modulation, Frequency Offset, Time-varying channel, Ultra-narrowband**

I. Introduction

Given that most WSN applications require low data rates, the ultra-narrowband communication scheme is emerging as a new approach to low data rate applications [1]–[3]. However, the carrier frequency offset (CFO) in such systems is a prominent challenge [3]. The CFO might be either the consequence of mismatch between local oscillators in the transmitter and the receiver or a Doppler shift caused by their relative movement. In [4], an autocorrelation based demodulator (ACD) for Double Differential PSK (DDPSK) has been proposed as an offset tolerant solution to tackle this issue. It removes the requirement of precise frequency generation which necessitates costly crystals and power hungry thermal compensations. In addition to frequency offset, the fading effect on such narrowband systems must be taken into account. As shown in [5], for a low data rate system a time-varying channel causes an error floor. This error floor is more drastic in ultra-narrowband systems due to a longer symbol time. As a consequence of time-varying behavior, channel estimation at the beginning of a packet is not reliable. Furthermore, using multiple pilot sequences for channel estimation imposes prohibitive overhead due to short packets used in these systems (as short as 200 symbols [3]).

In such circumstances diversity techniques can be utilized to improve performance [5]. Space diversity is dismissed because of low power and area constraints of the receiver. In a highly time-variant channel, time diversity (using channel coding and interleaving) is a possible solution. Additionally, frequency diversity (using frequency hopping) can be utilized. Nevertheless, both cases involve transmission of redundant information via channel coding. This increases either the bit rate or packet time. To keep the packet time constant (avoiding longer on-time for the RF front-end) for the same symbol rate, a higher order DDPSK can be used. The downside of the increased modulation order is a loss in BER performance. To avoid this performance loss hybrid frequency/phase modulation has been suggested [6]–[9]. Despite all research performed on different aspects of such a hybrid modulation, an offset tolerant demodulator which is capable of tolerating CFOs larger than the data rate has not been introduced. Besides, the error floor of such a hybrid modulation in a time-varying channel has not been dealt with in literature, though the performance of hybrid modulation in time-invariant (very slow) fading channels has been investigated [9].

The contribution of this work is twofold. First, an offset tolerant demodulator for a hybrid frequency/phase modulation is designed. Using such a demodulator a higher order modulation can be achieved with less performance loss compared to higher order DDPSK. Similar to [10], the performance of the demodulator is independent of CFO. Second, approximate error floor expressions are derived to show the benefit of the proposed demodulator in time-varying channel.

The rest of this paper is organized as follows. The next section elaborates on the design of the hybrid system for ultra-narrowband. Mathematical formulation and error floor expressions are presented in Section III. Simulation results and discussions are included in Section IV. Finally, Section V concludes the paper.

II. Design of Hybrid System for Ultra-Narrowband

As previously mentioned, the main target of demodulator design is to increase the modulation order while achieving a

978-1-5386-7646-2/19/$31.00 ©2019 IEEE

better BER performance compared to higher order DDPSK. For an ultra-narrowband application combining DDPSK with the smallest order of FSK (BFSK) is considered to minimize the increase in bandwidth and complexity of the demodulator. Assume that a basic system needs to transmit a packet of L information binary symbols with a symbol rate of R_s and the energy consumption for each of the L symbols is E_s. To design a modulator which compensates for the redundancy overhead, two requirements are considered. First, the packet time should remain constant (L/R_s) to avoid extra on-time of the node. Second, the energy consumption for each information binary symbol E_s and, as a result, the overall energy consumption which is required for transmitting L information symbols needs to remain constant. R_s is assumed to remain constant as well.

Now, we focus on the design of a hybrid system by combining Differential BFSK (DBFSK) and DDQPSK. This hybrid modulation is called BFQPSK in the following. Its modulation order is equal to 8 which is the same as the modulation order of DD8PSK. The increased modulation order provided by the hybrid modulation (or higher order modulation) can be used to apply any channel coding or diversity scheme for performance improvement. In this work, to compare the proposed demodulator for hybrid modulation and the conventional DDPSK demodulator, simple retransmission of symbols in different time intervals (repetition coding and interleaving) is considered as a use case scenario in time-varying channels. The proposed offset tolerant demodulator and conventional DD8PSK demodulator are simulated in such system to demonstrate achievable performance improvement.

A. Modulator Design

The baseband equivalent block diagram of the BFQPSK modulator is shown in Fig. 1. The data from the information source goes through channel coding (which is considered to be repetition code in this work). Then, bits are interleaved so that they are affected by uncorrelated channel characteristics. Afterwards, the interleaved sequence of bits is split between two different paths of FSK and PSK modulators. The ratio of the number of data bits passing through each path is proportional to the ratio of the number of bits in each PSK symbol to that of FSK symbol which is two in our case. Each symbol includes three bits, two modulated on QPSK and one on FSK. In the FSK branch the data is differentially encoded and sent to the FSK modulator while in the PSK branch data is coded with a double differential scheme. The modulated signals from each modulator are multiplied to form the final transmitter baseband signal.

B. Demodulator Design

The complex baseband model for the samples of the signal at the input of the demodulator during the n^{th} symbol assuming zero noise is as follows:

$$r_{k,n} = \sqrt{E_s/N_s}\exp[j((\omega_n+\omega_O)((n-1)T+kT_s)+\varphi_n)] \quad (1)$$

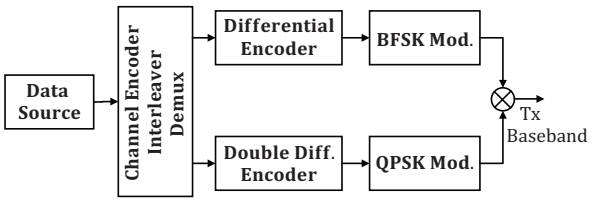

Fig. 1. Baseband equivalent block diagram of BFQPSK modulator

Where k is sample index, E_s is energy per symbol, N_s is the number of samples per symbol, T_s is sampling time, T is symbol period, ω_O is CFO, $\omega_n \in \{-\omega_d/2, +\omega_d/2\}$ (ω_d is frequency deviation of BFSK) and φ_n are information bearing frequency and phase, respectively. Frequency deviation (ω_d) is considered equal to $2\pi/T$. Applying a stage of the autocorrelation demodulator (ACD) to the signal similar to the DDPSK demodulator in [10], $X_{k,n}$ (samples of X_n) is achieved as follows.

$$\begin{aligned} X_{k,n} &= r_{k,n} r^*_{k,n-1} \\ &= \frac{E_s}{N_s}\exp[j(\Delta\omega_n kT_s + (\omega_{n-1}+\omega_O)T + \Delta\varphi_n)] \end{aligned} \quad (2)$$

where $\Delta\omega_n = (\omega_n - \omega_{n-1})$ and $\Delta\varphi_n = \varphi_n - \varphi_{n-1}$. Clearly, $\Delta\omega_n$ can have three different values, namely, 0 and $\pm\omega_d$. So in (2), the term $\Delta\omega_n(n+1)T$ is ignored as it is a multiple of 2π. Unlike the DDPSK demodulator, the frequency component is not removed at the output of the first ACD because the frequencies of two adjacent symbols might be different (depending on the FSK modulated data). It can be seen that the frequency component of $X_{k,n}$ only depends on FSK modulated data but not the CFO (ω_O). The modulated frequency ($\Delta\omega_n$) can be obtained using the Discrete Fourier Transform (DFT) of X_n as follows [11].

$$\Delta\hat{\omega}_n = \max_{\omega_i \in \Omega} |\mathcal{X}(j\omega_i)|^2, \quad (3)$$

where $\Omega = \{-\omega_d, 0, +\omega_d\}$ is the set of possible values of $\Delta\omega_n$ and $\mathcal{X}(j\omega_i)$ is the Discrete Fourier Transform of X_n. According to the definition of the DFT, for X_n we have:

$$\begin{aligned} \mathcal{X}_n(j\Delta\hat{\omega}_n) &= \sum_{k=0}^{N_s-1} X_{k,n}\exp[-j\Delta\hat{\omega}_n kT_s] \\ &= E_s\exp[j((\omega_{n-1}+\omega_O)T + \Delta\varphi_n)] \end{aligned} \quad (4)$$

In (4), the phase component includes two different terms, one depends on the modulated phase of two adjacent symbols ($\Delta\varphi_n$) and the other depends on the previous modulated frequency and CFO ($(\omega_{n-1}+\omega_O)T$). The offset dependent phase component can be eliminated by another differential detection similar to the second stage of the DDPSK demodulator in [10]. Let us define d_n as follows.

$$\begin{aligned} d_n &= \mathcal{X}_n(j\Delta\hat{\omega}_n)\mathcal{X}^*_{n-1}(j\Delta\hat{\omega}_{n-1}) \\ &= \exp(j(\Delta^2\varphi_n + \Delta\omega_{n-1}T)), \end{aligned} \quad (5)$$

where $\Delta^2\varphi_n = \Delta\varphi_n - \Delta\varphi_{n-1}$. As can be seen in (5) the phase component has again two terms. The first one is the double

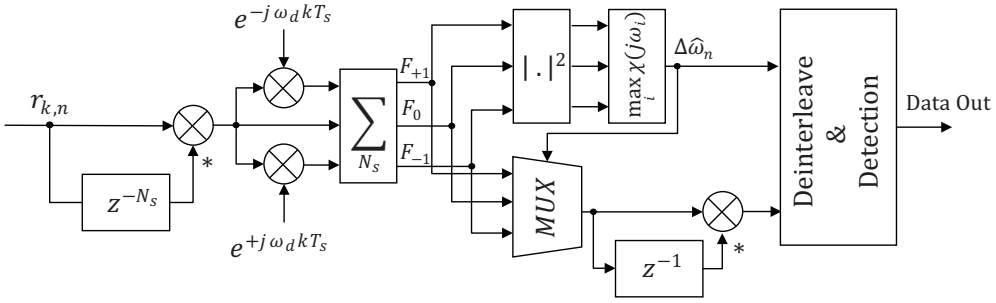

Fig. 2. The proposed offset tolerant demodulator for hybrid frequency/phase modulation

difference of signal phase over three consecutive symbols (the same difference used in DDPSK) and merely depends on the transmitted data over PSK. The second term, $\Delta\omega_{n-1}T$, can be ignored as it equals to an integer multiple of 2π. Using the assumption of $\omega_d = 2\pi/T$, eliminates the effect of $\Delta\omega_n(n+1)T$ and $\Delta\omega_{n-1}T$ on the phase in (2) and (5), respectively. Moreover, this assumption guarantees the best performance of the estimation in (3) and BFSK detection [11].

The block diagram of the demodulator based on (1)-(5) is depicted in Fig. 2. The received signal passes through an autocorrelation stage to achieve $X_{k,n}$ as in (2). Afterwards, samples $X_{k,n}$ are passed through three branches with different mixing coefficients in addition to a $\sum$ block, which are equivalent to the DFT of the signal at $\pm j\omega_d$ and 0. Then, the frequency component is detected according to the output of the MAX block. The result of the MAX block is also used to select the proper path which goes to the next stage of differential decoding. The outputs of the MAX block and the second ACD are sent to the de-interleaver and detection block to provide the transmitted data.

III. Error Floor Analysis

The improvement of hybrid modulation in an AWGN channel is demonstrated in literature [6]–[8]. In [9], the performance of the hybrid solution in flat-fading and a time-invariant Rayleigh fading channel is considered. However, the performance of a hybrid system in a time-varying channel has not been investigated. A time-varying channel implies that the received signal has a randomly varying phase. This is translated to a random frequency modulation which distorts the signal and leads to error even for $SNR = \infty$ [5]. This irreducible error is called error floor in this work.

In [12], the performance of simple receivers for FSK and PSK is considered and it is shown that, in contrast with DPSK, non-coherent FSK does not suffer from an error floor in time-varying channels. However, in the proposed demodulator for differential detection of FSK, signal passes through an autocorrelation stage (the multiplication with the conjugate of the delayed signal). As a consequence of this stage (as shown later), a time-varying fading channel causes an error floor in the proposed method for FSK detection. Nevertheless, in the sequel it is shown that the proposed offset tolerant FSK demodulator can still achieve a lower error floor compared to Double Differential PSK (DDPSK). As a result, the advantage of a hybrid solution (with our proposed demodulator) over higher order PSK also holds when the error floor in time-varying channels is considered. For mathematical derivations, a first order autoregressive model, AR(1), for fading channels is used [12], [13]. According to the previous section at the output of the first stage, the center frequency ranges from $-f_d$ to $+f_d$ (f_d is the frequency deviation of BFSK which is equal to the data rate in our system). Thus, a sampling rate of $4f_d$ (four samples per symbol) is considered for calculations to comply with the Nyquist criterion. The samples of the received signal in the n^{th} symbol period without any Gaussian noise ($SNR = \infty$) are as follows:

$$y_{k,n} = h_{k,n} r_{k,n}, k = 1, .., 4, \tag{6}$$

where $h_{k,n}$ and $x_{k,n}$ are the k^{th} sample of the complex channel gain and the transmitted signal during n^{th} symbol, respectively. Assuming an AR(1) model for the channel similar to [12], $h_{k,n}$ can be written in terms of its previous sample ($h_{k-1,n}$):

$$h_{k,n} = a h_{k-1,n} + \sqrt{1-a^2}\eta_{k,n}, \tag{7}$$

where $\eta_{k,n}$ is circularly symmetric white Gaussian noise $\mathcal{CN}(0, \sigma_h^2)$ and a is the normalized autocorrelation function of the channel, $R(\tau)$, for $\tau = T/4$ (sample time) in our formulation. Let $\boldsymbol{H} = [h_1, h_2, ..., h_8]$ denote the vector including all 8 samples of the channel gain over two consecutive symbols. Considering the first element equal to h and applying (7) recursively, element h_m of $\boldsymbol{H}$ (for $m = 2, 3, .., 8$) is obtained in terms of h.

$$\boldsymbol{H}(m) = h_m = a^{m-1}h + \sum_{i=1}^{m-1} a^{i-1}\sqrt{1-a^2}\eta_{m-i}, \tag{8}$$

where η_i ($i = 1, .., 7$) are independent $\mathcal{CN}(0, \sigma_h^2)$ random variables. The output of the first stage of the demodulator can be calculated as follows:

$$Y_{k,n} = y_{k,n} y^*_{k,n-1} = h_{k,n} r_{k,n} h^*_{k,n-1} r^*_{k,n-1} \tag{9}$$

Substituting h_k from (8) into (9) and ignoring terms including

$\eta_i\eta_j$ we achieve the following equations for $Y_{k,n}$, $k = 1, .., 4$:

$$Y_{k,n} = a^{2(k+1)}|h|^2 X_{k,n} + a^{k+3}\sum_{i=1}^{k-1} a^{i-1}\sqrt{1-a^2}h\eta^*_{m-i}X_{k,n} + a^{k-1}\sum_{i=1}^{k+3} a^{i-1}\sqrt{1-a^2}h^*\eta_{m-i}X_{k,n}, \quad (10)$$

where $X_{k,n} = r_{k,n}r^*_{k,n-1}$. The frequency component of X_n, ω_{X_n}, will have the value of zero if two consecutive BFSK symbols are the same. If symbols are different it will be $\pm\omega_d$ with a probability of 1/4 for each. According to (10), due to random variables η_i, $Y_{k,n}$ includes random terms in addition to signal component. Hereafter, for error floor calculations, these random terms are called noise and the ratio of signal power to the power of these random terms is referred to as SNR. As shown in Fig. 2, Y_n passes through three branches of filtering to achieve F_{-1}, F_0 and F_{+1} which are DFT values corresponding to $-\omega_d$, 0 and $+\omega_d$, respectively. Due to the X_n component in all noise terms and the correlation between random terms in samples of Y_n (resulting from the recursive nature of the channel model), the main part of the noise power is concentrated in the filter matched to the signal frequency ($\mathcal{X}_n(j\Delta\hat{\omega}_n)$) and the amount of noise in the adjacent filter is much smaller while the noise power in the non-adjacent filter (F_{+1} and F_{-1} are nonadjacent) is negligible. Therefore, the probability of error is as follows:

$$\begin{aligned} P_{e,BFSK} = 0.5[&P(|F_{+1}| > |F_0| \mid 0) + P(|F_{-1}| > |F_0| \mid 0)] \\ &+P(|F_0| > |F_{-1}| \mid -\omega_d)/4 \\ &+P(|F_0| > |F_{+1}| \mid +\omega_d)/4 \end{aligned} \quad (11)$$

All conditional probabilities in (11) are conditioned on the value of the frequency component at X_n i.e. $-\omega_d$, 0 and $+\omega_d$. These are cases leading to an error in non-coherent BFSK detection. So, each error probability in (11) is similar to the error probability for non-coherent BFSK [14]. However, there is a significant difference that must be taken into account. The conventional error probability function of non-coherent BFSK (based on matched filters [14]) is derived based on the assumption of equal noise power density in all filters which is not the case in our calculation according to the above mentioned facts (notice the explanation of (10)). This problem can be solved by calculating the noise power in the matched filter and the adjacent filter and recalculate the error probabilities using the modified noise power for each filter. Probabilities in (11) are the same and the mathematical derivation is continued for $P(|F_{+1}| > |F_0| \mid 0)$ for which we have [14]:

$$P(|F_{+1}| > |F_0| \mid 0) = \int_{|F_0|}^{\infty} f_{F_1}(x)dx = \exp(\frac{-|F_0|^2}{P_{n,+1}}) \quad (12)$$

where $f_{F_1}(x)$ is the probability density function (pdf) of $|F_{+1}|$. Since $\omega_{X_n} = 0$, the output of F_{+1} includes only Gaussian noise with variance equal to the noise power in F_{+1}. The envelope of F_{+1} has a Rayleigh distribution. According to expansion of (10) when $\omega_{X_n} = 0$, F_0 and F_{+1} are:

$$\begin{aligned} F_0 = &\sum_{k=1}^{4} a^{2(k+1)}|h|^2 + \sum_{m=1}^{4} a^{2-m}\sum_{k=1}^{4} a^{2k}\sqrt{1-a^2}h^*\eta_m \\ &+ \sum_{m=5}^{7} a^{m-6}\sum_{k=1}^{8-m} a^{2k}\sqrt{1-a^2}h^*\eta_m \\ &+ \sum_{m=1}^{3} a^{2-m}\sum_{k=m+1}^{4} a^{2k}\sqrt{1-a^2}h\eta^*_m \end{aligned} \quad (13)$$

$$\begin{aligned} F_{+1} = &\sum_{m=1}^{4} a^{2-m}\sum_{k=1}^{4}(-j)^k a^{2k}\sqrt{1-a^2}h^*\eta_m \\ &+ \sum_{m=5}^{7} a^{m-6}\sum_{k=1}^{8-m}(-j)^{k+1} a^{2k}\sqrt{1-a^2}h^*\eta_m \\ &+ \sum_{m=1}^{3} a^{2-m}\sum_{k=m+1}^{4}(-j)^k a^{2k}\sqrt{1-a^2}h\eta^*_m \end{aligned} \quad (14)$$

where η_m are independent $\mathcal{CN}(0, \sigma_h^2)$ random variables and the signal component of F_{+1} is ignored. As a result of the $X_{k,n}$ component in (10), there is an E_s factor in both the signal and noise terms. As it does not affect SNR, it is normalized in (13)-(14) and the undergoing formulations. Thus, the signal power in F_0 and noise power in F_0 and F_{+1} (all normalized to E_s) are as follows.

$$P_S = S|h|^4 \quad (15)$$

$$P_{N,0} = \Gamma_0(1-a^2)|h|^2\sigma_h^2 \quad (16)$$

$$P_{N,+1} = \Gamma_{+1}(1-a^2)|h|^2\sigma_h^2 \quad (17)$$

where:

$$\begin{aligned} \Gamma_0 = &\sum_{m=1}^{4}|a^{2-m}\sum_{k=1}^{4} a^{2k}|^2 + \sum_{m=5}^{7}|a^{m-6}\sum_{k=1}^{8-m} a^{2k}|^2 \\ &+ \sum_{m=1}^{3}|a^{2-m}\sum_{k=m+1}^{4} a^{2k}|^2 \end{aligned} \quad (18)$$

$$\begin{aligned} \Gamma_{+1} = &\sum_{m=1}^{4}|a^{2-m}\sum_{k=1}^{4}(-j)^k a^{2k}|^2 \\ &+ \sum_{m=5}^{7}|a^{m-6}\sum_{k=1}^{8-m}(-j)^{k+1} a^{2k}|^2 \\ &+ \sum_{m=1}^{3}|(a^{2-m}\sum_{k=m+1}^{4}(-j)^k a^{2k}|^2 \end{aligned} \quad (19)$$

To calculate noise power, the terms $h^*\eta_m$ are considered to be independent $\mathcal{CN}(0, |h|^2\sigma_h^2)$ random variables. Using values in (15)-(17) and following the same procedure as in [14] for conventional non-coherent BFSK, the following equation for error probability in terms of instantaneous $SNR = P_S/(P_{N,+1} + P_{N,0})$ can be obtained.

$$P_e = \frac{P_{N,+1}}{P_{N,+1} + P_{N,0}}\exp(-\frac{P_S}{P_{N,+1} + P_{N,0}}) \quad (20)$$

Considering a Rayleigh fading channel and calculating average SNR (over h) and average error probability according to [15], we achieve $\overline{P_e}$ as:

$$\overline{P_e} = \frac{(1-a^2)\Gamma_0}{(1-a^2)(\Gamma_0+\Gamma_{+1})+S} \tag{21}$$

Thus, the error floor (EF_{DBFSK}) is obtained by substituting (21) into (11).

$$EF_{DBFSK} = \frac{3}{2}\frac{(1-a^2)\Gamma_0}{(1-a^2)(\Gamma_0+\Gamma_{+1})+S}, \tag{22}$$

where a is $J_0(2\pi\upsilon_{max}T/4)$ for a Rayleigh fading channel with a maximum Doppler shift of υ_{max}.

Now, we need to calculate the error floor for DDBPSK. In DDBPSK demodulator signal after the first stage is equal to F_0. Notice that in DDBPSK $X_{k,n}$ is constant over the whole symbol period. Based on (10), (13) and (18), the signal at the input of the second stage of differential detection (Y_n) is as follows.

$$Y_n = \sqrt{S}|h|^2 X_n + \sqrt{\Gamma_0(1-a^2)|h|^2}X_n\Lambda_n, \tag{23}$$

where Λ_n is a $\mathcal{CN}(0,\sigma_h^2)$ random variable. Using (15) and (16) it is easy to show that for Y_n, $SNR = P_s/P_{N,0}$. This is used as the input of the next differential detector. Applying the same method as [12] and [15] for DPSK and averaging SNR over h for a Rayleigh channel, the probability of error for DDBPSK is obtained as follows.

$$EF_{DDBPSK} = \frac{\Gamma_0(1-a^2)}{2\Gamma_0(1-a^2)+2S}, \tag{24}$$

where a is $J_0(2\pi\upsilon_{max}T/4)$ for a Rayleigh fading channel with a maximum Doppler shift of υ_{max}. Fig. 3 demonstrates the error floor for different values of maximum Doppler shift in a Rayleigh fading channel with Jakes Doppler spectrum. The solid lines show values obtained from (22) and (24) while dashed lines are simulation results. It can be seen that the theoretical and simulation results are in agreement while there is a slight difference for the higher values of υ_{max}. In our approximations the multiplication of noise terms is ignored. This assumption does not hold for large values of Doppler shift which increases the variance of random component in (7). Thus, as υ_{max} increases, the theory slightly deviates from simulations. Fig. 3 demonstrates that the error floor achieved by DBFSK using the proposed demodulator is lower than the one can be obtained by the conventional DDBPSK. Increasing the modulation order of DDPSK is equivalent to using a higher order DPSK with an input equal to (23) which leads to even higher error. As a result, if modulation order is increased by hybrid modulation, the error floor will be lower compared to increasing the order of DDPSK.

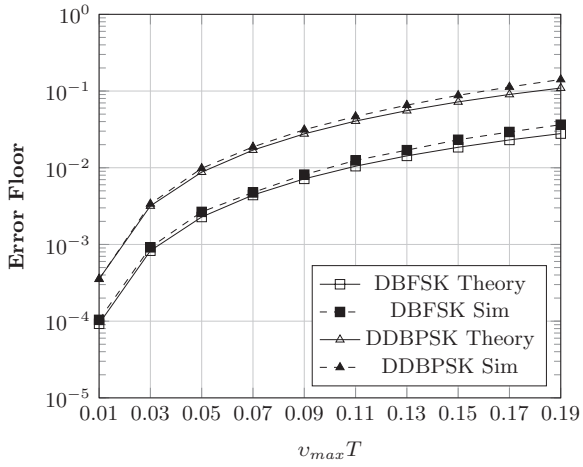

Fig. 3. Simulated and theoretical error floor versus normalized maximum Doppler shift in a Rayleigh fading channel with Jakes Doppler spectrum

IV. Simulation Results and Discussion

As mentioned before, to evaluate the performance a simple repetition coding is used for simulations. Using 8PSK or a combination of BFSK and QPSK, instead of BPSK, increases modulation order to eight. Thus, using a rate-1/3 repetition coding is possible while packet time is kept constant for the same symbol rate. Considering the requirements mentioned in section II, the energy per symbol remains the same as in the BPSK case. Thus, for QPSK and 8PSK $E_b = 1/2E_s$ and $E_b = 1/3E_s$, respectively. In other words, going from BPSK to QPSK and 8PSK (higher orders of modulation) adds more replicas of each information binary symbol but decreases energy per each replica proportionally. As a consequence the BER performance in AWGN channel is not different from the uncoded case. In contrast, in the BFQPSK method modulator order is increased by adding another orthogonal dimension instead of higher order PSK modulation. The new replica of information binary symbol is transmitted by changing the frequency of the same signal which is carrying QPSK. As a result the energy per each new replica is E_s. To clarify, going from BPSK to BFQPSK, three replicas of information binary symbols are transmitted among which two have $E_b = 1/2E_s$ and one has $E_b = E_s$. This means that E_b is effectively higher in case of BFQPSK compared to both QPSK and 8PSK and that is why the performance of BFQPSK is better in AWGN channel. This performance improvement is achieved at the expense of increased bandwidth. Considering the low data rate and ultra-narrowband signal, the loss of bandwidth is affordable and outweighed by the performance improvement.

In the following simulations, the symbol rate is considered to be 100 Sym/s (similar to [3]) and the sampling frequency is 8 times of data rate ($N_s = 8$). Fig. 4 demonstrates the BER curve of the DD8PSK and BFQPSK in an AWGN channel. The improvement of BFQPSK compared to 8PSK at $BER = 10^{-3}$ (which is more than $5dB$) shown in [6] is preserved also in the proposed offset tolerant demodulator. As can be seen, BFQPSK is better than DDQPSK except for very low E_s/N_0 region. The main reason of higher error rates in low E_s/N_0 region is the dependence of QPSK detection on DFSK detection in the proposed demodulator. However, in higher SNR, BER decreases faster than DDQPSK due to higher effective E_b. The robustness to CFO is illustrated in Fig. 5 where the BER values at $E_s/N_0 = 12, 14\ dB$ are shown

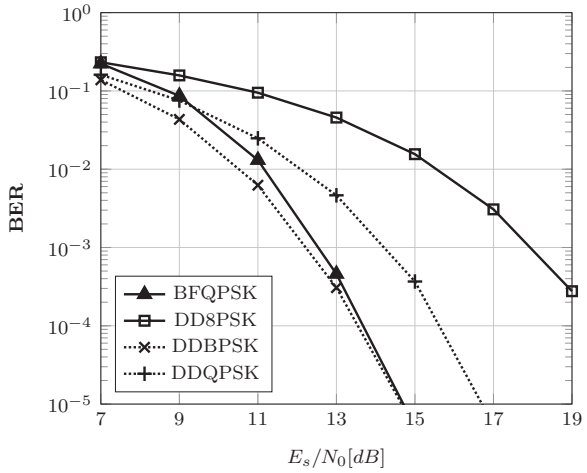

Fig. 4. BER performance of DDBPSK, DDQPSK, DD8PSK and BFQPSK in AWGN channel

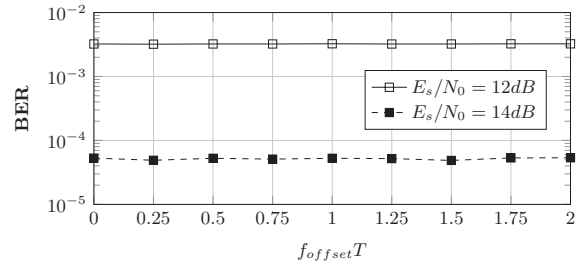

Fig. 5. BER for BFQPSK in AWGN for CFO values normalized to symbol rate

for different values of CFO.

Simulation results for Rayliegh fading channel, which is the worst case scenario, are presented here. The BER performance in Rician channel varies between the BER in a Rayleigh channel and an AWGN channel depending on the K factor. However, for sake of brevity BER curves are not included.

Fig. 6 depicts the BER of the proposed demodulator and the conventional DD8PSK demodulator in a Rayleigh fading channel with a Jakes Doppler spectrum and $\upsilon_{max}T = 0.02$. For better comparison the DDBPSK in AWGN and the same fading channel are shown as well. It can be seen that the proposed demodulator improves the BER performance considerably compared to DD8PSK. At $BER = 0.001$ the proposed method achieves $4\ dB$ improvement.

V. Conclusion

The problem of the time-varying channel and CFO were considered simultaneously for ultra-narrowband communications. To overcome the effect of a time-varying channel, diversity techniques together with channel coding can be exploited. However, the transmission of redundant data leads to an increase in packet duration. To keep packet duration unchanged for a constant symbol rate, the order of modulation needs to increase. To avoid performance loss resulting from higher order PSK, a hybrid frequency/phase scheme was selected. To tackle the CFO problem in ultra-narrowband systems an offset tolerant demodulator for such a hybrid

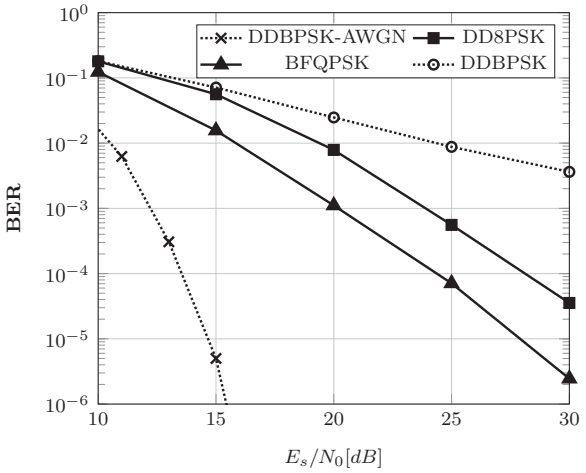

Fig. 6. BER curves in Rayleigh channel with $\upsilon_{max}T = 0.02$

scheme was proposed. The designed demodulator which is a combination of DBFSK and DDQPSK outperforms DD8PSK by $4\ dB$ at $BER = 0.001$ in a Rayleigh fading channel with normalized maximum Doppler shift equal to 0.02.

References

[1] K. E. Nolan, W. Guibene, and M. Y. Kelly, "An evaluation of low power wide area network technologies for the internet of things," in *2016 International Wireless Communications and Mobile Computing Conference (IWCMC)*, Conference Proceedings, pp. 439–444.

[2] [Online]. Available: https://www.sigfox.com/en

[3] D. Lachartre, F. Dehmas, C. Bernier, C. Fourtet, L. Ouvry, F. Lepin, E. Mercier, S. Hamard, L. Zirphile, S. Thuries, and F. Chaix, "7.5 a tcxo-less 100hz-minimum-bandwidth transceiver for ultra-narrow-band sub-ghz iot cellular networks," in *2017 IEEE International Solid-State Circuits Conference (ISSCC)*, ISSCC, Conference Proceedings, pp. 134–135.

[4] S. Safapourhajari and A. B. J. Kokkeler, "Demodulation of double differential psk in presence of large frequency offset and wide filter," in *2018 IEEE 87th Vehicular Technology Conference (VTC Spring)*, siavash, Conference Proceedings, pp. 1–5.

[5] A. Molisch, *Wireless Communications*. Wiley, 2012.

[6] I. Ghareeb, "Bit error rate performance and power spectral density of a noncoherent hybrid frequency-phase modulation system," *IEEE Journal on Selected Areas in Communications*, vol. 13, no. 2, pp. 276–284, 1995.

[7] W. Lei and I. Korn, "Combined frequency and differential phase shift keying with non-coherent detection in a satellite mobile channel," *IEEE Transactions on Vehicular Technology*, vol. 44, no. 3, pp. 603–612, 1995.

[8] C. Char-Dir, "Differential detection of quadrature frequency/phase modulated signals," *IEEE Transactions on Communications*, vol. 47, no. 4, pp. 546–557, 1999.

[9] I. Ghareeb and A. Yongacoglu, "Performance of joint frequency phase modulation over rayleigh fading channels," *IEE Proceedings - Communications*, vol. 141, no. 4, pp. 241–247, 1994.

[10] M. K. Simon and D. Divsalar, "On the implementation and performance of single and double differential detection schemes," *IEEE Transactions on Communications*, vol. 40, no. 2, pp. 278–291, 1992.

[11] S. Hara, A. Wannasarnmaytha, Y. Tsuchida, and N. Morinaga, "A novel fsk demodulation method using short-time dft analysis for leo satellite communication systems," *IEEE Transactions on Vehicular Technology*, vol. 46, no. 3, pp. 625–633, 1997.

[12] K. S. Gomadam and S. A. Jafar, "Modulation and detection for simple receivers in rapidly time-varying channels," *IEEE Transactions on Communications*, vol. 55, no. 3, pp. 529–539, 2007.

[13] K. E. Baddour and N. C. Beaulieu, "Autoregressive modeling for fading channel simulation," *IEEE Transactions on Wireless Communications*, vol. 4, no. 4, pp. 1650–1662, 2005.

[14] S. Haykin, *Digital Communication Systems*. Wiley, 2013.

[15] S. Stein, "Fading channel issues in system engineering," *IEEE Journal on Selected Areas in Communications*, vol. 5, no. 2, pp. 68–89, 1987.